Published in final edited form as:
Mol Inform. 2015 August 20; 34(11-12): 709–714. doi:10.1002/minf.201500089.

Attractors in Sequence Space: Peptide Morphing by Directed Simulated Evolution

Jan A. Hiss[#*,a], **Katharina Stutz**[#a], **Gernot Posselt**[b], **Silja Weßler**[b], and **Gisbert Schneider**[*,a]

[a]Swiss Federal Institute of Technology (ETH), Department of Chemistry and Applied Biosciences, Vladimir-Prelog-Weg 4, CH-8093 Zurich, Switzerland [b]Paris-Lodron University of Salzburg, Department of Molecular Biology, Division of Microbiology, Billroth Str. 11, 5020 Salzburg, Austria

[#] These authors contributed equally to this work.

Keywords

antimicrobial peptide; evolutionary algorithm; lipid membrane; mitochondrial targeting; peptide design

Certain antimicrobial peptides (AMPs) and mitochondrial targeting peptides (mTPs) share common features such as a positive net charge, helical propensity, and the ability to interact with lipid membranes[1]. While a primary function of AMPs is to disrupt membrane integrity, many mTPs interact with the mitochondrial membranes and the translocator complex, leaving the membranes intact when proteolytically degraded by matrix-located protease(s)[2]. We present a computational approach that may help rationalize the delicate balance of these effects and other sequence-activity relationships. We implemented and applied a directed evolutionary strategy for stepwise peptide morphing of one peptide into another (MoPED, *Morphing of Peptides by Evolutionary Design*). For the prospective application, we chose cationic peptides as representatives of both peptide classes and converted an AMP (Protonectin, start sequence)[3] into an mTP (target or “attractor” sequence). Novel peptides were generated based on a chemical similarity index (Grantham substitution matrix).[4] The target sequence served as an attractor point for evolutionary exploration of sequence space. We synthesized and tested the individual peptides that were generated during the morphing process. The designed peptides showed systematic loss of membranolytic potential with increasing distance from the start sequence. The results of biophysical and bacterial growth experiments confirmed the applicability of MoPED to designing chemically motivated peptide derivatives. Receiver operating characteristic

[*]Fax: +41 44 633 13 79, Tel: +41 44 633 74 38 gisbert.schneider@pharma.ethz.chjan.hiss@pharma.ethz.ch.

Conflict of Interest
None declared.

Europe PMC Funders Author Manuscripts

(ROC) analysis advocates the inducible peptide α-helicity as a semi-quantitative indicator of membranolytic antimicrobial activity.

In the early 1990s Schneider and Wrede pioneered the concept of evolutionary peptide design and optimization by *Simulated Molecular Evolution* (SME).[5] The original SME method relies on the (μ, λ) evolution strategy,[6] which means that μ parent peptides (μ≥1) are modified by residue mutation to obtain a set of λ new peptides constituting a "generation". The mutation operator does not vary or shuffle the residue symbols in a random fashion, but is based on a well-motivated physicochemical similarity principle.[7] To define the degree of sequence variation by a mutation, *i.e*. the Shannon entropy of the residue distribution among the offspring,[8] a pairwise similarity index s_{ij} between residues *i* and *j* is computed. With decreasing pair-wise similarity (≡increasing distance in sequence space), residue *i* is substituted by residue *j* with a decreasing probability. In SME, the residue transition probability P(*i*→*j*) is computed as a normalized exponential (Eq. (1)).

$$P(i \rightarrow j) = exp\left(-\frac{s_{ij}^2}{2\sigma^2}\right) / \sum_j exp\left(-\frac{s_{ij}^2}{2\sigma^2}\right). \quad (1)$$

According to this mutation model, the pair-wise amino acid similarity values are used to obtain *pseudo*-probabilities for each residue position in a peptide (Figure 1). This concept results in a non-symmetric residue substitution matrix, so that forward and reverse mutations can have different transition probabilities, P(*i*→*j*)≠P(*j*→*i*). The width σ of the approximately bell-shape distribution of offspring around the parent is a so-called strategy parameter (adaptive memory) during peptide evolution, which itself underlies selection, thereby enabling automated fitness-dependent adaptation of function-altering and neutral mutations.[9,10]

MoPED builds on the SME principle. The two main differences to the original algorithm are:

- **i.** The stochastic algorithm is equipped with an attractor sequence ("target" or "end" sequence), which means that starting from the initial parent sequence offspring is generated in an iterative mutation-selection cycle until the target sequence has been obtained.
- **ii.** The algorithm performs a directed stochastic walk in sequence space.

New sequences were generated by help of the Grantham matrix, which captures the pair-wise amino acid exchange based on composition and physicochemical properties, specifically residue polarity and molecular volume.[4] Grantham distances (so-called "biochemical distances") are in statistically significant agreement with observed evolutionary transition probabilities.[4,11] The distance concept pursued in this study does not represent the only solution to computing physicochemical similarities, as there are several related approaches, *e.g*. the Grantham matrix derived measure of Miyata *et al*.[12] and the experimentally obtained exchangeability matrix approach of Yampolsky and Stoltzfus.[11] The results of a MoPED run will critically depend on the substitution matrix used, particularly for skewed residue compositions.[13] In MoPED, stepwise mutations

morph the start sequence into the target (end) sequence. Here, we pursued a (1, λ) mutation-selection strategy, so that each iteration resulted in a new intermediate sequence (the "fittest" of each generation). The aspect of directed evolution was achieved by evaluating the fitness of the newly generated sequence as their Grantham distance to the attractor sequence (Figure 2). We wish to stress that the algorithm does not attempt to mimic a biological evolution process; it merely borrows the mutation-selection principle from evolution theory as a means for performing an adaptive walk through sequence space.[5]

For ease of synthesis, we omitted peptides that contained methionine or cysteine, and used 12-mers as start and attractor sequences. The AMP Protonectin (**1**, ILGTILGLLKGL) served as the start sequence and the mTP from mitochondrial hydroxyacylglutathione hydrolase (**16**, VVGRGLLGRRSL, UniProt: GLO2_HUMAN, residues 2–13) as attractor sequence for the first MoPED run (run 1, σ_{Start} = 0.5). This setting directed the simulated evolution gradually away from the AMP towards the mTP. We investigated the loss of membranolytic function by automated sequence morphing. We performed two consecutive runs with our algorithm (run 1 and run 2): Run 1 (σ_{Start} =0.5, λ=10) was meant to cover the whole distance between the AMP and the mTP (Table 1, sequences **1**–**16**), run 2 (σ_{Start} =0.1, λ=5) emphasized the immediate sequence neighborhood around Protonectin (Table 1, sequences **i1**–**i12**). The individual steps of the sequence morphing process of run 2 are shown in Figure 3.

We synthesized all peptides using Fmoc solid phase synthesis on robotic synthesizers. The purified peptides (>90% UV_{210}) were tested in concentrations of 1 μM and 10 μM on large unilamellar vesicles (LUVs, ∅=1 μm) composed of different lipid compositions (POPEG, POPC, POPCECL containing 5% or 20% cardiolipin, respectively) to determine their direct membranolytic activity (Table 1).[14,15] We performed circular dichroism (CD) spectroscopy to identify the peptides' inducible alpha helical content by transfer from an aqueous (pure water) to a hydrophobic environment (trifluoroethanol (TFE):water mixture), and additionally measured the peptides' capacity to inhibit the growth of the Gram-positive bacterium *Staphylococcus aureus*.

The results obtained (Table 1) demonstrate successful morphing of the start AMP into the attractor mTP. We observed a stepwise alteration of membranolytic activity and selectivity. In run 1 the morphing process generated 14 sequences (**2**–**14**, Table 1), with the AMP being the start and the mTP being the end sequence. The membrane-disruptive activity of the start sequence was confirmed as well as the hitherto putative non-disruptive activity of the end sequence. With the exception of peptide **2** none of the intermediate sequences from run 1 possessed membranolytic capacity (Table 1). Peptide **2** showed mild rupturing (50–75%) of POPC vesicles but lost activity on all other vesicles and *S. aureus* compared to its parent Protonectin. We concluded that the initial step-size σ_{Start} (width of the *pseudo*-probability function, Figure 1) was too large in run 1 and thus performed run 2 with (i) a smaller σ_{Start} value and (ii) more similar start and end sequences, to further increase the resolution around Protonectin by favoring smaller residue alterations. In fact, the peptides generated by MoPED run 2 (**i1**–**i12**) all have a smaller Grantham distance to Protonectin than peptide **2** from run 1 (*D*=297).

With a single conservative L→I mutation peptide **i1** exhibited reduced activity (10 μM) on POPC and POPCECL20% compared to Protonectin **1** (1 μM) but possessed the same overall selectivity/activity pattern (Table 1). A smooth transition according to the Grantham distance matrix apparently allows for a smooth transition with respect to activity and selectivity ("Principle of Strong Causality"[6,10]). This tendency continues with peptides **i2**–**i10** for which we observed diminished overall membranolytic potential and activity on fewer LUV types with increasing distance to Protonectin. A particularly informative example is peptide **i3**, which is further away from Protonectin (*D*=113) than its immediate neighbors **i2** (*D*=22) and **i4** (*D*=69) but lost all activity, while **i2** and **i4** retained function. A possible explanation for the loss of activity of **i3** could be the F→A mutation in position eight. This peptide might lie on an "activity cliff", which argues for a non-concentric activity realm around Protonectin. This interpretation is supported by peptides **i7** (*D*=136) and **i8** (D=167), which still show activity on POPC but reside further apart from Protonectin in sequence space compared to **i3** (*D*=113). Obviously the naïve assumption of a linear distance-dependent loss of function is unwarranted. Inaccuracies of the fitness function are at least partially alleviated by the stochastic sequence generation concept implemented in MoPED. Apparently, the peptide activity space, although presumably complex in its structure, is sufficiently well sampled by our algorithm.

The algorithm generated sequences that represent a smooth transition from the AMP towards the mTP, but also obtained sequences lying at the edge of the activity space and possessing varying selectivity. We expect this effect to originate from the directed evolutionary process. The presence of an attractor results in a directed and therefore straightforward movement through the peptide activity landscape (Figure 2).

Although POPC vesicles do not mimic bacterial membranes, the peptide-induced rupture of POPC membranes (>75%) matched the observed bactericidal effects on *S. aureus*, with the exception of **i8**. The apparent preference for POPC membranes is in line with observations made for AMPs of the aurein and maculatin families and may be explained by mechanistic aspects of peptide-membrane insertion.[15,16]

By using CD spectroscopy we measured the inducibility of α-helicity, which has been suggested to correlate with membranolytic potential.[17] This previous observation is corroborated by the results of our study. The peptides with a four-fold (or greater) helix inducibility during the transition from water to a hydrophobic environment (1/1 eq. TFE/water) competently inhibited growth of *S. aureus in vitro* (Table 1). In fact, inducible α-helicity might thus be useful as an easily accessible and quantifiable indicator of membranolytic peptide activity. For our controlled data set we obtained a close-to-perfect ROC area under the curve of 0.99 when treating the *S. aureus* results (Table 1) as true positives.

Conclusions

The results of this study provide evidence for the usefulness of directed peptide evolution by computational peptide morphing. In extension to former evolutionary peptide design approaches we incorporated an attractor sequence and therefore an aspect of directed

evolution. In MoPED the evaluation of the designed sequences ("fitness measure") is not based on biochemically determined activity, but on computed distances towards the attractor peptide which allows for smooth transition steps between the start and target peptides and an informative exploration of fitness space. Thereby, it complements full-deck virtual peptide screening.[18] The main idea behind the MoPED approach is to generate a first choice of reference peptides. The concept might assist in the design of minimalist peptide libraries for rapid exploration of sequence-activity relationships and fitness landscape modeling.[19] Here we successfully designed sequences with gradually modulated activity and selectivity towards four different membrane types as well as *S. aureus*. Membranolytic activity non-linearly decreased with increasing distance from the start sequence. Whether this observation is a consequence of the peptide representation used or a general property of the antimicrobial sequence space will be subject of a separate investigation. Irrespective of the outcome of these studies, our results point to inducible α-helicity and related peptide properties as critical for the bactericidal effect of AMPs.

Experimental Section

Peptide synthesis and analytics

All peptide sequences were synthesized by 9-fluorenylmethoxycarbonyl (Fmoc) solid-phase peptide synthesis on automated parallel peptide synthesizers (Symphony™ and Prelude™, Protein Technologies, USA) using 200 mM Rink amide 4-methyl benzhydrylamine (MBHA) resin (AAPPTec, USA) (0.52 mmol/g) as solid support. Amino acids were purchased from AAPPTec or Protein Technologies and dissolved in dimethylformamide (DMF) (Sigma-Aldrich, USA). The peptides were treated with 20% pyrrolidine (Acros Organics, USA) in DMF (v/v) to deprotect the resins and the amino acids. Amino acids were subsequently coupled to the resin-bound peptides using 200 mM O-(6-chlorobenzotriazol-1-yl)-*N*,*N*,*N*',*N*'-tetramethyluronium hexafluorophosphate (HCTU) (Protein Technologies, USA) and 400 mM N-methylmorpholine (NMM) (Fisher Chemical, USA) as coupling reagents. After coupling of the terminal amino acids, the peptides were washed with DMF and dichlormethane (DCM) (Sigma-Aldrich, USA) and cleaved from the resin by a mixture of 95% trifluoracetic acid (TFA) (ABCR, Germany), 2.5% triisopropylsilane (TIS) (Sigma-Aldrich, USA) and 2.5% ddH_2O (v/v/v). The peptides were precipitated with diisopropyl ether (Fluka, Switzerland) at −20°C over night, centrifuged (for 10 min at −10°C and 3000 rpm) and re-suspended for five-cycles in ice-cold diisopropyl ether and dried under ambient atmosphere for three days. The crude peptides were purified using reverse-phase preparative HPLC (Shimadzu, Japan) on a Nucleodur C18 HTec column (150×21 mm, 5 um, 110 Å) with a linear 5–70% acetonitrile (Sigma-Aldrich, USA) in water gradient containing 0.1% formic acid (Merck Millipore, Germany) and a flow rate of 0.5 ml/min (at 40°C and 120 mbar). Detection was performed by UV spectroscopy at a wavelength of 210 nm. Peptide purity was analyzed by UV detection and electrospray mass detection using analytical reverse-phase HPLC-MS on a Nucleodur C18 HTec column (150×3 mm, 5 um, 110 Å) and identical conditions as for preparative HPLC. The Purified peptides were lyophilized at 0.03 mbar and −85°C using an Alpha 2-4 LDplus Freeze Dryer (Christ, Germany).

Preparation of lipid vesicles (LUVs)

1-palmitoyl-2-oleoyl-*sn*-glycero-3-phosphocholine (POPC), 1-palmitoyl-2-oleoyl-*sn*-glycero-3-phosphoethanolamine (POPE), 1-palmitoyl-2-oleoyl-*sn*-glycero-3-phospho-(1′-rac-glycerol) (sodium salt) (POPG) and cardiolipin (CL) from bovine heart (sodium salt) were purchased as dry powders from Avanti Polar Lipids (Alabaster, AL, USA) and stored as 20 mg/ml stock solutions dissolved in chloroform (≥99.8%, Sigma-Aldrich, USA). For LUV production the lipids were weighed in and combined in corresponding ratios (POPC: 1 eq., POPE/POPG: 6.9/3.1 eq., POPC/POPE/CL20%: 4.5/3.5/2 eq., POPC/POPE/CL5%: 5.2/3.8/1 eq.). Lipid combinations containing POPE were preheated at 40°C. A dry lipid film was formed by successive evaporation of chloroform. The lipids were rehydrated in 3 ml of 1 M TRIS at pH 7.4 (trizma hydrochloride solution, Sigma-Aldrich, USA) and 3 ml of 36 mM carboxyfluorescein in TRIS pH 7.4 (5(6)-carboxyfluorescein ≥ 95% (HPLC), Sigma-Aldrich, USA). Vesicle formation was accomplished by ten cycles of freeze cooling using liquid nitrogen and a 40 °C water bath. A defined vesicle size was achieved by extruding vesicles 19 times through a polycarbonate membrane (pore size ∅=1 μm) in a Mini Extruder (Avanti Polar Lipids). To remove free carboxyfluorescein solution, the vesicles were purified on Sephadex DNA-Grade Illustra NAP-25 columns (GE Healthcare, UK). An ascorbic acid method was used for the determination of the final phospholipid concentrations.[20]

Vesicle rupture assay

The membrane rupturing potential of peptides was investigated as the percentage of released carboxyfluorescein in relation to the amount of released dye after addition of Triton X-100. Peptide solutions in concentrations of 100 μM and 10 μM were mixed in a v :v ratio of 1 :9 with an 11 μM solution of each vesicle type filled with carboxyfluorescein dye, resulting in final peptide concentrations of 10 μM and 1 μM, respectively. Additional peptide samples were prepared containing either 1% Triton X-100 (100% membrane rupturing potential) as positive control, and water (0% membrane rupturing potential) as negative control. Immediately after sample preparation, carboxyfluorescein dye leakage was measured as fluorescence intensity on an Infinite M1000 Microplate Reader (Tecan, Switzerland). The samples were measured in triplicate at 24.5 °C and at excitation/emission wavelengths of 490/520 nm.

Circular dichroism spectroscopy

A Chirascan CD Spectrometer (Applied Photophysics, UK) was used for measuring CD spectra of peptides. Using a 1 mm thick glass cuvette (Helma Analytics, Type No. 110-QS), peptide concentrations of 50 μM were measured in water and in a 2,2,2-trifluorethanol (99.8% extra pure, Acros Organics, USA)/water mixture (1/1 eq.). Near-UV measurements were performed in triplicate and a scanning range from 180 nm to 260 nm with a step size of 1 nm. Each measurement resulted in 243 raw data points. By the help of the Pro-Data Viewer software (Applied Photophysics, UK, version 4.2.15), triplicate measurements were averaged, baseline subtracted and smoothed (window size=4). The analyses of the resulting spectra were conducted using the DichroWeb service portal[21] and by applying the CONTIN algorithm with reference set 3.[22]

Bacteria and real-time growth monitoring

S. aureus SH1000 expressing GFP was a gift from Phil Hill (The University of Nottingham, UK) and was cultured on tryptic soy agar (Sigma-Aldrich, Germany) containing 10 μg/ml chloramphenicol. For monitoring bacterial growth, 1×10^6 bacteria were incubated in 200 μl nutrient broth containing 10 mg/ml chloramphenicol and 50 μM peptide solution in transparent Nunclon™ Edge 96-well plates (SIFIN GmbH, Germany). The plates were shaken for 20 h at 37°C in a M200 PRO Quad4 Monochromators™-based multimode reader (Tecan, Anif, Austria). Loading the plate moats with 4×3 ml of 0.1% agarose reduced evaporation of the culture medium. Growth was monitored by detecting the fluorescence signal of GFP (Ex 485/9 nm, Em 535/20 nm) and OD_{600nm} every two hours.

Acknowledgements

Sarah Haller and Daniel Reker are thanked for technical support and discussion. This research was supported by the Swiss National Science Foundation (grant no. 200021_157190 to G. S. and J. A. H.), the ETH Zurich (ETH Research Grant ETH-01 12-1 to G. S.), and the Austrian Science Fund (FWF grants P_24074 and P_24315 to S. W.).

Abbreviations

AMP	antimicrobial peptide
CD	circular dichroism
CL	cardiolipin
LUV	large unilamellar vesicle
mTP	mitochondrial targeting peptide
POPC	1-palmitoyl-2-oleoyl-*sn*-glycero-3-phosphocholine
POPE	1-palmitoyl-2-oleoyl-*sn*-glycero-3-phosphoethanolamine
POPG	1-palmitoyl-2-oleoyl-*sn*-glycero-3-phospho-(1′-rac-glycerol)
SME	simulated molecular evolution
TFE	trifluoroethanol

References

[1] a). Lee TH, Hall KN, Aguilar MI. Curr. Top. Med. Chem. 2015 in press. b) Fjell CD, Hiss JA, Hancock RE, Schneider G. Nat. Rev. Drug Discov. 2011; 11:37–51.c) Hancock RE, Sahl HG. Nat. Biotechnol. 2006; 24:1551–1557. [PubMed: 17160061]

[2] a). Dudek J, Rehling P, van der Laan M. Biochim. Biophys. Acta. 2013; 1833:274–285. [PubMed: 22683763] b) Merklinger E, Gofman Y, Kedrov A, Driessen AJ, Ben-Tal N, Shai Y, Rapaport D. Biochem. J. 2012; 442:381–389. [PubMed: 22142226] c) Gebert N, Ryan MT, Pfanner N, Wiedemann N, Stojanovski D. Biochim. Biophys. Acta. 2011; 1808:1002–1011. [PubMed: 20696129] d) Hildenbeutel M, Habib SJ, Herrmann JM, Rapaport D. Int. Rev. Cell. Mol. Biol. 2008; 268:147–190. [PubMed: 18703406] e) Maduke M, Roise D. Science. 1993; 260:364–367. [PubMed: 8385804] f) Ståhl A, Pavlov PF, Szigyarto C, Glaser E. Biochem. J. 2000; 349:703–707. [PubMed: 10903130]

[3]. Baptista-Saidemberg NB, Saidemberg DM, de Souza BM, César-Tognoli LM, Ferreira VM, Mendes MA, Cabrera MP, Ruggiero Neto J, Palm MS. Toxicon. 2010; 56:880–889. [PubMed: 20600225]

[4]. Grantham R. Science. 1974; 185:862–864. [PubMed: 4843792]

[5] a). Schneider G, Wrede P. Biophys. J. 1994; 66:335–344. [PubMed: 8161687] b) Schneider G, Schrödl W, Wallukat G, Müller J, Nissen E, Rönspeck W, Wrede P, Kunze R. Proc. Natl. Acad. Sci. USA. 1998; 95:12179–12184.

[6] a). Bayer H-G, Schwefel H-P. Natural Computing. 2002; 1:3–52.b) Rodrigo G, Carrera J, Elena SF. Biochimie. 2010; 92:746–752. [PubMed: 20399826] c) Rechenberg, I. Evolutionsstrategie – Optimierung technischer Systeme nach Prinzipien der biologischen Evolution. Frommann-Holzboog; Stuttgart: 1973.

[7] a). Schneider G, Schuchhardt J, Wrede P. Biophys. J. 1995; 68:434–447. [PubMed: 7696497] b) Schneider G, Schuchhardt J, Wrede P. Comput. Appl. Biosci. 1994; 10:635–645. [PubMed: 7704662]

[8]. Zuegge J, Ebeling M, Schneider G. J. Mol. Graph. Model. 2001; 19:304–306. 379. [PubMed: 11449568]

[9]. Hiss, JA.; Schneider, G. De Novo Molecular Design. Schneider, G., editor. Wiley-VCH; Weinheim: 2013. p. 441-470.

[10]. Schneider, G.; So, S-S. Adaptive Systems in Drug Design. Landes Bioscience; Georgetown: 2001.

[11]. Yampolsky LY, Stoltzfus A. Genetics. 2005; 170:1459–1472. [PubMed: 15944362]

[12]. Miyata T, Miyazawa S, Yasunaga T. J. Mol. Evol. 1979; 12:219–236. [PubMed: 439147]

[13]. Altschul SF, Wootton JC, Gertz EM, Agarwala R, Morgulis A, Schäffer AA, Yu YK. FEBS J. 2005; 272:5101–5109. [PubMed: 16218944]

[14] a). Blondelle SE, Lohner K, Aguilar M. Biochim. Biophys. Acta. 1999; 1462:89–108. [PubMed: 10590304] b) Teixeira V, Feio MJ, Bastos M. Prog. Lipid Res. 2012; 51:149–177. [PubMed: 22245454]

[15]. Sani MA, Henriques ST, Weber D, Separovic F. J. Biol. Chem. 2015 in press.

[16]. Cheng JT, Hale JD, Elliott M, Hancock RE, Straus SK. Biochim. Biophys. Acta. 2011; 1808:622–633. [PubMed: 21144817]

[17]. Lin Y-C, Hiss JA, Schneider P, Thelesklaf P, Lim YF, Pillong M, Koehler FM, Dittrich P, Halin C, Wessler S, Schneider G. ChemBioChem. 2014; 15:2225–2231. [PubMed: 25204788]

[18]. Fjell CD, Jenssen H, Cheung WA, Hancock RE, Cherkasov A. Chem. Biol. Drug Des. 2011; 77:48–56. [PubMed: 20942839]

[19] a). Schneider G, Schuchhardt J, Wrede P. Biol. Cybern. 1995; 73:245–254. [PubMed: 7548312] b) Schneider G, Wrede P. Prog. Biophys. Mol. Biol. 1998; 70:175–222. [PubMed: 9830312]

[20]. Chen PS, Toribara TY, Warner H. Anal. Chem. 1956; 28:1756–1758.

[21]. Whitmore L, Wallace BA. Biopolymers. 2008; 89:392–400. [PubMed: 17896349]

[22] a). Provencher SW, Glockner J. Biochemistry. 1981; 20:33–37. [PubMed: 7470476] b) Greenfield NJ. Nat. Protoc. 2006; 1:2876–2890. [PubMed: 17406547]

Europe PMC Funders Author Manuscripts

Europe PMC Funders Author Manuscripts

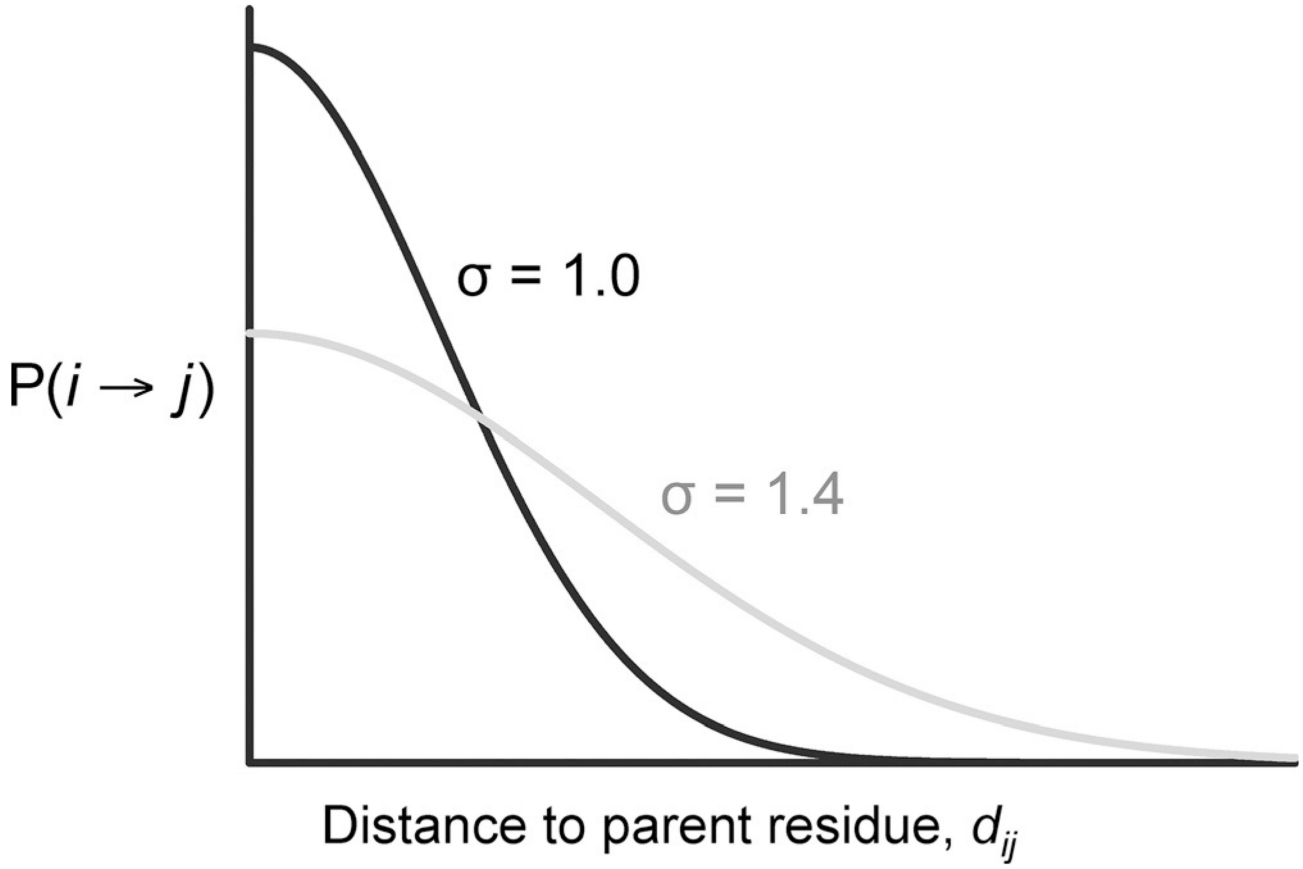

Figure 1.

Distance-based residue mutation. The idealized graph shows *pseudo*-probability functions *P* for residue mutations $i \rightarrow j$, with widths σ=1.0 and 1.4, centered at the parent residue *i* (*d*=0). The chance for observing the transition $i \rightarrow j$ decreases with the distance between residues *i* and *j*, d_{ij}. The choice of s influences the residue diversity (entropy) of the mutated sequence.

Europe PMC Funders Author Manuscripts

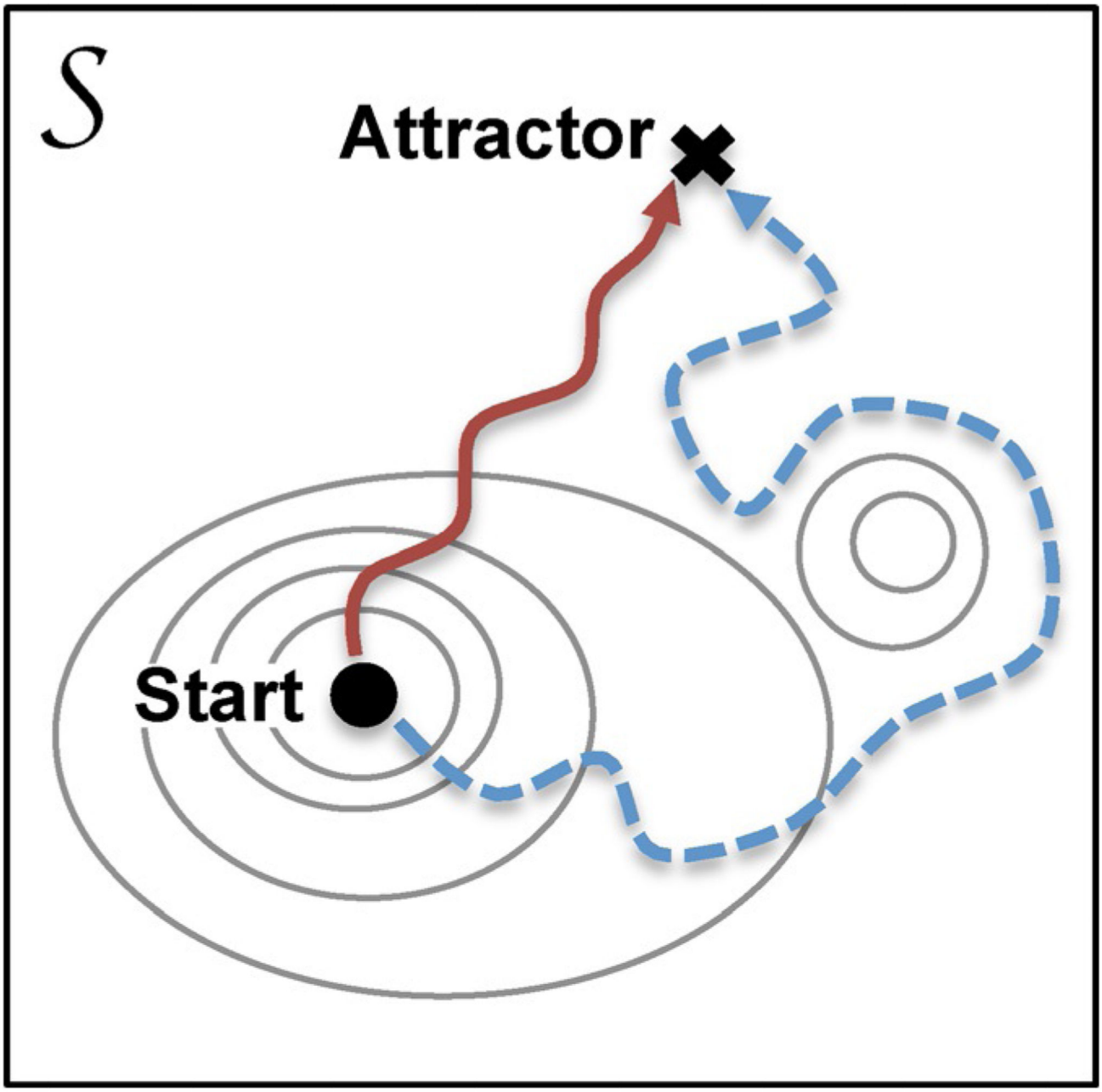

Figure 2.

Schematic of directed (red arrow) vs. undirected (blue, dashed arrow) evolutionary stochastic search in peptide sequence space *S*. Contour lines represent an observable quality index (*e.g*. membranolytic potential). In the simplifying example both search processes follow a path towards lower quality index values (*e.g*. loss of membranolytic potential). The directed approach limits the degrees of freedom of movement by adding an attractor (target sequence) to the search process.

Europe PMC Funders Author Manuscripts

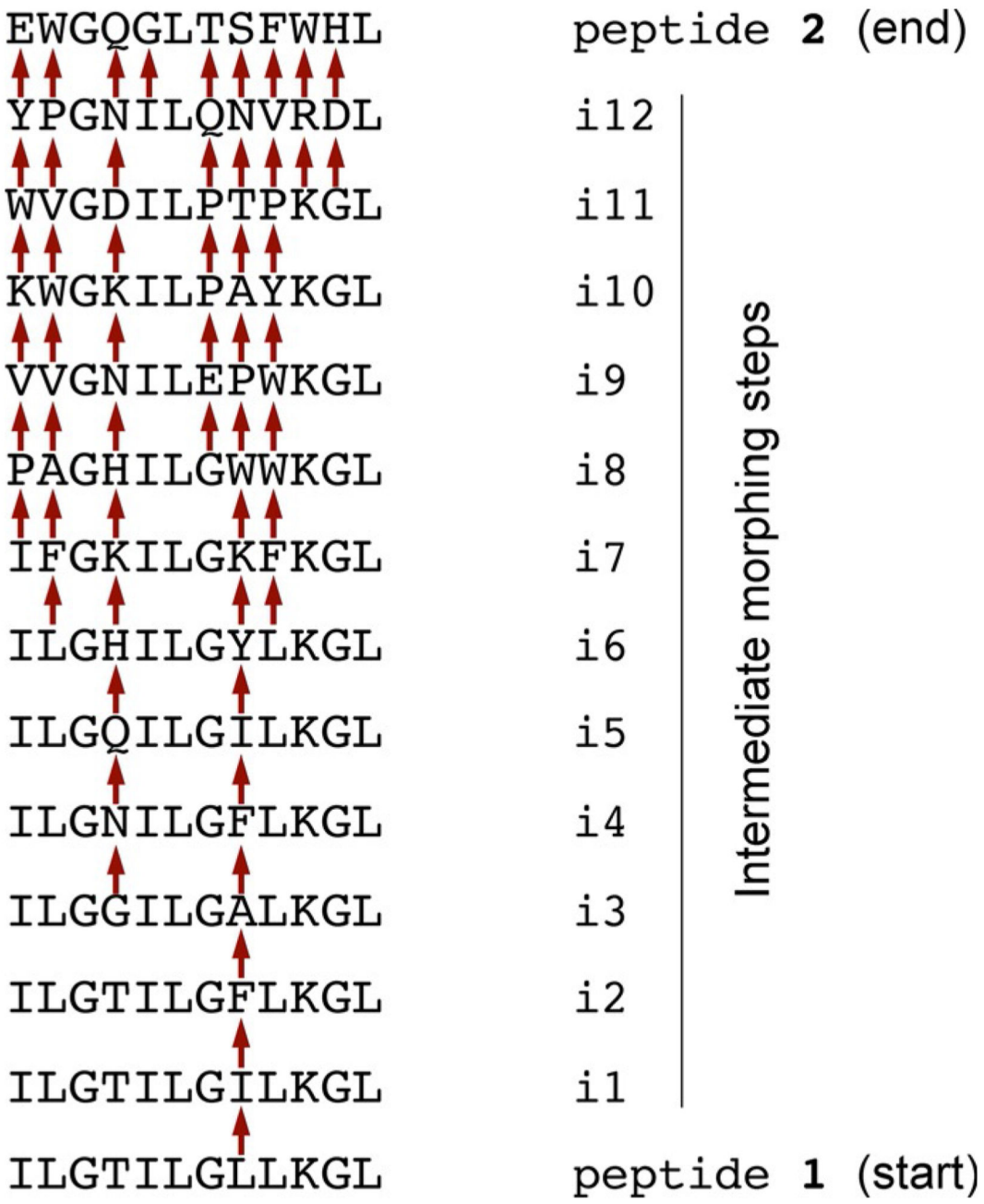

Figure 3.

Schematic of the morphing procedure of MoPED run 2 resulting in 12 intermediate peptides (ID: **i1**–**i12**). The arrows designate the mutated amino acid residues in the respective morphing step. The sequences shown correspond the “fittest” offspring in each generation (λ=5). The Grantham distance *D* to the target sequence (peptide **2**) served as the fitness function (here: minimization problem) for peptide selection.

Table 1

Activity of the peptides generated in MoPED run 1 (ID: **1**–**16**) and run 2 (ID: **i1**–**i12**). *D*: Distance to the start peptide Protonectin (**1**) according to the Grantham matrix. ✓: LUV disruptive capacity ≥75% compared to Triton (=100%), or bacterial growth inhibition (10^6 *S. aureus*) over 20 h; (✓) LUV disruptive capacity ≥50% and <75%. Empty fields: LUV disruptive capacity <50%, or no bacterial growth inhibition. Fold α-helix induction was measured by CD spectroscopy.

ID	Sequence	*D*	Vesicle (LUV) type								*S.aureus* growth inhibition [50 μM]	Fold α-helix induction (TFE/H_2O) [50 μM]
			POPC		POPCE CL 5%		POPCE CL 20%		POPEG			
			Peptide concentration / μM									
			10	1	10	1	10	1	10	1		
1	ILGTILGLLKGL	0	✓	(✓)	(✓)		(✓)	(✓)	(✓)		✓	4
i1	ILGTILGILKGL	5	✓		(✓)		✓		(✓)		✓	4.8
i2	ILGTILGFLKGL	22	✓	(✓)	✓		(✓)		(✓)		✓	4.4
i3	ILGGILGALKGL	113										3.4
i4	ILGNILGFLKGL	69	✓								✓	3.7
i5	ILGQILGILKGL	42	✓				(✓)				✓	6.3
i6	ILGHILGYLKGL	59	✓				(✓)				✓	4.5
i7	IFGKILGKFKGL	136	(✓)				(✓)					3.8
i8	PAGHILGWWKGL	167	✓				(✓)					2.2
i9	VVGNILEPWKGL	170										1.5
i10	KWGKILPAYKGL	180	(✓)				(✓)					1.8
i11	WVGDILPTPKGL	178										1.6
i12	YPGNILQNVRDL	238										2.2
2	EWGQGLTSFWHL	297	(✓)									1.4
3	VPGWGLYTTTDL	314										1.7
4	VVGKGLYDTDSL	315										1.5
5	VVGQGLWGHKSL	296										1.7
6	VVGHGLFGEHSL	297								✓		1.7
7	VVGVGLFGDHSL	318										1.7
8	VVGFGLPGRFSL	275										1.4
9	VVGKGLPGRQSL	252										1
10	VVGHGLFGRTSL	290										2.4
11	VVGWGLWGRESL	326										1.3
12	VVGVGLYGRESL	287										1
13	VVGEGLYGRQSL	285										1.9
14	VVGQGLLGRPSL	290										1.4
15	VVGHGLLGRKSL	272										1.8
16	VVGRGLLGRRSL	278										1.8